Journal of the European Ceramic Society 20 (2000) 2353–2366

Spinel forming ceramics of the system $Fe_xNi_yMn_{3-x-y}O_4$ for high temperature NTC thermistor applications

Adalbert Feltz *, Walter Pölzl [1]

Electronic Parts and Components Keramische Bauelemente, EPCOS KB, Siemensstraße 43, A-8530 Deutschlandsberg, Austria

Received 14 September 1999; received in revised form 17 April 2000; accepted 29 April 2000

Abstract

The thermal stability and aging of spinels of the system Fe_2O_3–NiO–Mn-oxide are studied by measuring the electrical properties of ceramic samples obtained by sintering up to 1350°C. Based on the formula $Fe_x^{III}Ni_y^{II}Mn_{3-x-y}^{z}O_{3+x/2+\delta}$, chemical analyses of ceramic samples with defined values of x and y make it possible to determine the average oxidation number z of manganese with $z = [2\delta/(3-x-y)] + 2$ thus leading to the share of oxygen $[(2-x-2\delta)/4]$ O_2 which is liberated during sintering. X-ray diffraction measurements of samples with higher NiO and lower Fe_2O_3 content indicate NiO separation. Hence, the analytical results are suitable to elucidate the phase constitution of the ceramics consisting of a mixture of NiO and of a spinel with modified composition. The formation of the spinel ceramics $FeNi_{0.5}Mn_{1.5}O_4$ ($x = 1$, $y = 0.5$) and $FeNi_{0.7}Mn_{1.3}O_4$ ($x = 1$, $y = 0.7$) in a single-phase state, i.e. without oxygen loss on sintering at 1350 or 1300°C in air, is due to the lower content of NiO at a sufficiently high fraction of Fe_2O_3 in the composition. The compounds show ferrimagnetic behavior. $FeNi_{0.5}Mn_{1.5}O_4$ has a Curie temperature of 245 5°C. At increasing temperature, commonly above 150°C or 200°C up to 400°C the specific electrical resistivity $\rho_{25°C}$ and the value of the $B_{25/100°C}$ constant of both of the two compounds depend on time and on the thermal pre-treatment of the samples. Aging is due to the frozen-in state of the equilibrium of distribution of cations between the tetrahedral and octahedral sites of the spinel structure. This tends to shift towards equilibrium when the temperature is increased step by step during aging; it can be followed by measuring the electrical properties. The changes are observed to arise approaching the Curie temperature. Soaking of the samples at 650°C after aging for 72 and 144 h up to 500°C shows that the variations of the $\rho_{25°C}$ and $B_{25/100°C}$ values can be repeated in a following aging cycle, provided that the same cooling rate is applied. On the other hand, above 400 °C the ralaxation effects fail. Changes in this range of higher temperature involve fast rates of cation re-distribution thus leading to short waiting times until a constant value of the electrical resistivity is achieved. Hence, above 400°C, $FeNi_{0.5}Mn_{1.5}O_4$ ceramics appear completely stable against aging within common measuring times. Therefore, they should be suitable for high temperature NTC thermistor applications. The comparatively high value $B_{25/100°C} = 7470$ K makes it possible to measure the temperature via the electrical resistivity with satisfactory sensitivity, e.g. $\alpha = 1/\rho(d\rho/dT) = 0.8\%$ is achieved in the range around 750°C.

Keywords: Crystal structure; Electrical properties; Fe(Ni, Mn)$_2O_4$; NTC; Spinels; Thermistors

Zusammenfassung

Es wird über die thermische Stabilität der im System Fe_2O_3–NiO–Mn-Oxid zugänglichen Spinelle und das Alterungsverhalten der elektrischen Eigenschaften von Keramikproben berichtet, die durch Sintern an der Luft bei 1300 bis 1350°C erhalten werden. Ausgehend von der Zusammensetzung $Fe_x^{III}Ni_y^{II}Mn_{3-x-y}^{z}O_{3+x/2+\delta}$ mit $z = [2\delta/(3-x-y)] + 2$ wird aus der chemischen Analyse von Proben mit bestimmten Werten für x und y die mittlere Oxydationstufe z des Mangans ermittelt und damit zugleich auf den Anteil Sauerstoff $[(2-x-2\delta)/4]$ O_2 geschlossen, der bei der Sinterung freigesetzt wird. Auf Grund von röntgenographischen Untersuchungen sind die Analysenergebnisse bei den Proben mit höherem NiO — und zugleich vergleichsweise geringem Fe_2O_3 — Gehalt auf eine NiO-Ausscheidung zurückzuführen, d. h. es liegt eine mehrphasige Keramik mit bestimmtem Anteil an NiO und einer Spinellphase vor, deren Zusammensetzung entsprechend verändert ist. Eine Ausnahme bilden die Spinelle $FeNi_{0.5}Mn_{1.5}O_4$ ($x = 1$, $y = 0.5$) und $FeNi_{0.7}Mn_{1.3}O_4$ ($x = 1$, $z = [2\delta/(3-x-y)] + 2 = 0.7$), deren NiO–Gehalt zugunsten des Fe_2O_3 — Gehalts vermindert ist. Derartige Halbleiterkeramiken lassen sich bei 1350 bzw. 1300°C an Luft unzersetzt sintern. Die Verbindungen sind ferrimagnetisch. $FeNi_{0.5}Mn_{1.5}O_4$ hat eine Curie- Temperatur von 245 5°C. Beide Verbindungen weisen im Temperaturbereich bis zu

* Corresponding author. Tel.: +43-3462-800-2410; fax; +43-3462-800-373.

E-mail address: adalbert.feltz@siemens.dlb1.de or adalbert.felt3@apcos.com (A. Feltz).

[1] Present address: Austria Mirkro Systeme International AG, AMS, Schloß Premstätten, A-8141 Unterpremstätten, Austria.

0955-2219/00/$ - see front matter
PII: S0955-2219(00)00140-0

400°C eine von der thermischen Vorbehandlung stark beeinflußte Zeitabhängigkeit der spezifischen elektrischen Leitfähigkeit $\rho_{25°C}$ und der $B_{25/100°C}$- Konstante auf. Auf Grund der nachgewiesenen Phasenhomogenität kann das Alterungsverhalten auf temperaturabhängige Gleichgewichte der Verteilung der verschiedenen Kationen auf den Tetraeder und Oktaederplätzen der Spinellstruktur zurückgeführt werden, die oberhalb der Curie - Temperatur verstärkt einsetzen. Ausgehend von einer Äquilibrierung bei 650°C und anschließender definierter Abkühlung sind die Alterungswerte zyklisch wiederholbar. Oberhalb 400°C entfallen die Relaxationseffekte, da die Einstellung der inneren Gleichgewichte bei einer Temperaturänderung dann rasch erfolgt und sich eine für den praktischen Anwendungsfall hinreichend kurze Wartezeit bis zur Einstellung eines konstanten Widerstandswertes ergibt. Davon ausgehend stellt $FeNi_{0.5}Mn_{1.5}O_4$ oberhalb 400°C eine alterungsstabile Keramik dar, die auf Grund ihrer hohen B–Konstante von 7470 K in Hochtempertur–Thermistoren mit hinreichender Empfindlichkeit, z. B bei 750°C mit $\alpha = 1/\rho(d\rho/dT) = -B/T^2 = 0.8\%$, anwendbar ist.

1. Introduction

Changing of the electrical properties with time, particularly when the temperature is increasing, appears as an essential reason for limiting the application of oxide ceramic NTC thermistors to temperatures below 150 or 200°C.[1] On the other hand, special devices with glass covered oxide ceramics have been developed yielding comparatively permanent electrical data up to 400°C.[2,3] In a steel or platinum encapsulated version even higher temperatures of application have been described, e.g. for exhaust gas temperature sensing up to 1000°C.[3,4] Nevertheless, the reliability of the electrical data of NTC ceramics submitted to long term high temperature exposure is still unsatisfactory.

Aging of the electrical properties results from non-equilibrium states which exist inherently in available semiconducting NTC ceramics. Preferentially, spinel forming oxide systems are used based on manganese oxide in combination with NiO and/or CoO/Co_3O_4, Fe_2O_3 and/or Cu_2O/CuO. Commonly, sintering in air at a sufficiently high temperature has to be applied for achieving densification. However, at those conditions heterogeneous materials are often formed consisting of two or more phases, whose ratio and composition depend on the sintering temperature and on the cooling rate. In part oxygen loss takes place at the high sintering temperature leaving behind a mixture of a rocksalt type phase and a spinel phase with modified composition. The fraction as well as the oxidation state and cation vacancy concentration of the different phases depend sensitively on the temperature of sintering and on cooling. Depending on the cooling rate, different equilibria occur on quenching. $NiMn_2O_4$ decomposes above 950°C in air by oxygen cleavage yielding NiO and a residual spinel with changed composition.

$$NiMn_2O_4 \rightarrow a\,NiO + a/6\,O_2 + \frac{3-a}{3}\,Ni_{3\frac{(1-a)}{3-a}}Mn_{\frac{6}{3-a}}O_4 \quad (1)$$

Sometimes, as for $NiMn_2O_4$ the spinel phase is only formed in fast cooling from higher temperature. At slow cooling, oxygen is absorbed below 730°C initiating separation into two phases. αMn_2O_3 and the ilmenite type compound $NiMnO_3$ are formed.[5]

$$2NiMn_2O_4 + 1/2O_2 \rightleftarrows \alpha Mn_2O_3 + NiMnO_3 \quad (2)$$

Moreover, for homogeneous spinel phases the internal equilibria of cation exchange between the crystallographically distinct tetrahedral and octahedral sites have to be taken into consideration.[6] The quenched states of all of these incompletely equilibrated reactions can be a source of aging. Variations of the electrical properties with time have to be expected when the temperature of quenching of one of these reactions is close to the range of temperature where thermistor application takes place.

Consequently, semiconducting ceramics consisting of a compound with definite composition and structure showing no decomposition or phase transformation from sintering down to room temperature have been suggested as more suitable for thermistors. In such a single phase ceramic, aging of the electrical properties should be significantly reduced. Hence, provided that the requirement of sufficient sensitivity is obeyed, high temperature applications become more available. According to the relation

$$\rho(T) = \rho_{25°C}\exp[E_A/RT] = \rho_{25°C}\exp[B/T] \quad (3)$$

thermistor sensitivity α is defined by $\alpha = 1/\rho(d\rho/dT) = -B/T^2$. Therefore, as an additional prerequisite for high temperature thermistor applications comparatively high values of the B constant are required even if the condition of zero or small aging is met.

The present paper concerns NTC ceramics of the system Fe_2O_3–NiO–Mn-oxide.

Earlier studies[7] in the series $Fe_xNiMn_{3-x}O_4$ had shown that single-phase spinel compounds are formed as a result of thermal decomposition of mixed crystal oxalate powders $Fe_xNi_yMn_{3-x-y}(C_2O_4)_3{\cdot}6H_2O$ yielding first of all a defect spinel, which makes sintering possible already at about 1000°C. However, densification of the ceramic samples remained incomplete. On the other

hand, sintering at higher temperatures implies phase separation providing NiO and a spinel with changed composition. Starting from mixed crystal oxalate precursor powders, Martinez et al.[8] report also the formation of single-phase spinel compounds in the range of lower NiO content of the Fe_2O_3–NiO–Mn-oxide system using sintering temperatures up to 1300°C.

It is the aim of the present paper to extend these studies in order to elucidate the reasons for aging and to find a solution for high temperature applications. In the system $Fe_xNi_yMn_{3-x-y}O_4$ the upper limit of thermal stability is suggested to increase when the y value is decreasing. Therefore, the mixed oxide preparation technique and sintering at 1300 or 1350°C, followed alternatively also by soaking at 1000°C, have been applied.

2. Spinel formation and thermal stability

Fig. 1 shows the range of spinel formation near room temperature for the system $Fe_xNi_yMn_{3-x-y}O_4$ after sintering in air.[9] Large areas of phase separation prevail.

On the left hand side, the high temperature solid state spinel solutions of Mn_3O_4, Fe_3O_4 and $NiFe_2O_4$ are submitted to oxidation in air when the temperature is decreasing. In dependence on composition different shares of α Fe_2O_3 and α Mn_2O_3 are separated and at the same time a residual NiO containing spinel is formed, which is stable against oxidation in air. Phase separation in the system $(Ni_{1-x}Fe_x)O$ in dependence on oxygen partial pressure has been studied by Ricoult and Schmalzried.[10]

On the right-hand side of the figure, the position of the cubic spinel $NiMn_2O_4$ ($a_0 = 839.7$ pm) is indicated, which is unstable at room temperature. Obviously, the widely inversed cation distribution coupled with Mn^{II} formation on the tetrahedral sites in the result of Mn^{III} disproportionation according to $[Ni^{II}_{0.1}Mn^{II}_{0.9}]^{[4]}[Ni^{II}_{0.9}Mn^{IV}_{0.9}Mn^{III}_{0.2}]^{[6]}O_4$[11–14] gives rise for a driving force of oxygen contamination followed by decomposition according to Eq. (2). However, as we have shown for $Fe_{1/6}NiMn_{11/6}O_4$ ($a_0 = 838.8$ pm),[6] the gap of instability can be closed by addition of relatively small shares of Fe_2O_3 in the series $Fe_xNiMn_{2-x}O_4$. Fe^{III} prefers tetrahedral site

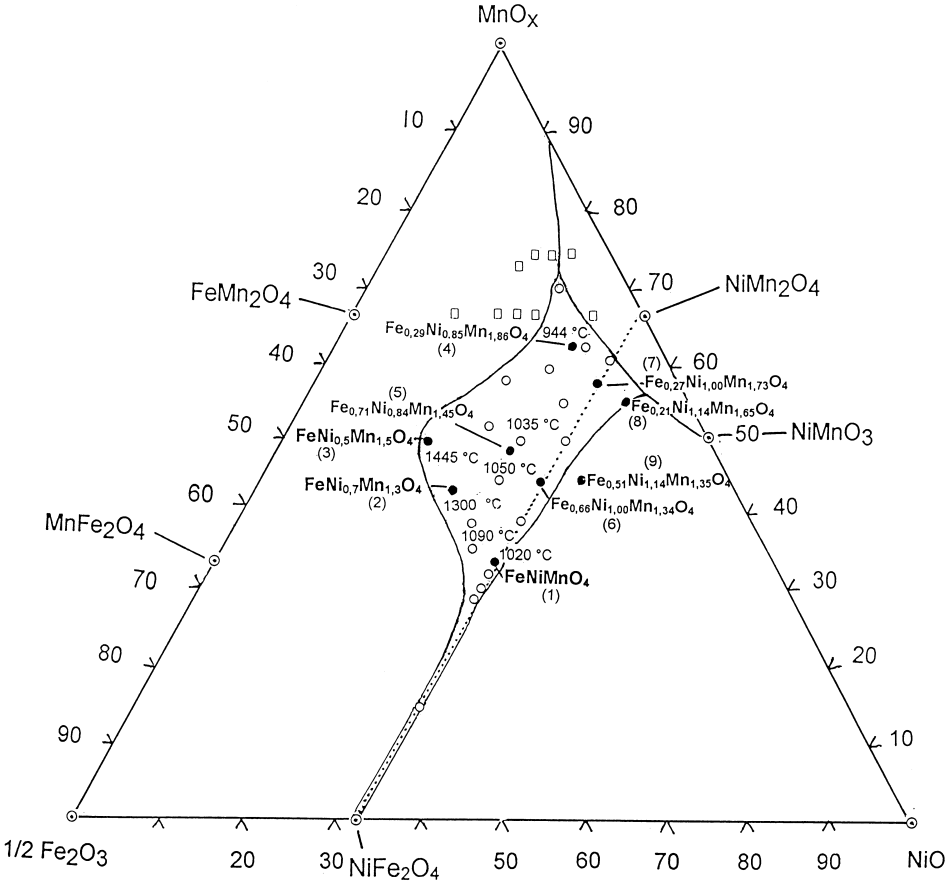

Fig. 1. Spinel formation area of the system $Fe_xNi_yMn_{3-x-y}O_4$ near room temperature in air and temperature of decomposition from DTA measurement: (○) samples prepared yielding the single-phase spinel state provided that preparation starts from the mixed crystal oxalate precursor $Fe_xNi_yMn_{3-x-y}(C_2O_4)_3{\cdot}6\ H_2O$, however being with the exception of sample (2) and (3) partially decomposed when the mixed oxide preparation route is applied; (●) samples whose electrical properties and aging has been measured; (□) samples which even by application of the precursor route could not be obtained in the homogeneous spinel state.

occupation in the spinel structure allowing the Ni^{II} cations to enter the preferred octahedral sites. Hence, Mn^{II} formation as a the result of Mn^{III} disproportionation is reduced thus leading for $x \geqslant 1/6$ to the formation of spinel compounds which are stable against oxidation in air.

However, preparation of samples along the dotted line $y = 1$ and $1/6 < x < 1$, i.e. between $NiMn_2O_4$ and $NiFe_2O_4$, requires a mixed crystal oxalate precursor $Fe_xNiMn_{2-x}(C_2O_4)_3.6H_2O$, which can be transformed into a defect spinel powder by thermal decomposition in air.[15] Sintering activity of this precursor powder is increased thus making possible sintering of pressed pellets already at about 1000°C.[6] Application of higher sintering temperatures leads to NiO separation according to

$$Fe_xNiMn_{2-x}O_4 \rightarrow aNiO + a/6O_2 + \frac{3-a}{3}Ni_{\frac{3x}{3-a}}Fe_{3\frac{(1-a)}{3-a}}Mn_{\frac{3(2-x)}{3-a}}O_4 \quad (4)$$

This reaction is detectable by DTA measurements. The decomposition proceeds the more the higher the temperature of sintering. As shown by the values of the reaction on-set temperature noticed inside the spinel formation area of Fig. 1, the thermal stability is increasing for higher Fe content and lower Ni content in the spinel phase. Hence, the most steep increase of thermal stability is observed in the series $FeNi_yMn_{2-y}O_4$ ($x = 1.1 > y > 0.5$). Indeed, an approach to the composition of $FeNi_{0.5}Mn_{1.5}O_4$ makes it possible to obtain single-phase spinels by sintering even at a temperature $T > 1350$°C. Therefore, reasonably the familiar mixed oxide preparation route has been used.[16]

3. Preparation of ceramics in the system $Fe^{III}_xNi^{II}yMn^z_{3-x-y}O_{3+x/2+\delta}$

The preparation has started from mixtures of Ni^{II}-oxide, Fe^{III}-oxide and Mn-oxide or of suitable basic carbonates, whose metal contents have been accurately determined by analyes. The weighed components were ball milled in an aqueous slurry for 24 h using agate spheres. After evaporation of the water, drying and sieving, for calcination the powder mixture was heated to 750°C for 4 h. The procedure of ball milling, drying and sieving has been repeated followed by a second step of thermal treatment, this time at 850°C for 4 h. The powder was then ground up to about 1.2 μm using Y_2O_3 hardened ZrO_2 spheres of 1 cm for 4 h and in a second step by spheres of 1 mm in diameter for 1 h. After granulation using a polyvinyl alcohol binder, cylindrical pellets have been formed by pressing. For metallization these green bodies were coated on opposite sides using a Pt paste. After sintering the samples had a diameter of about 3.0 mm and a height of about 1.3 mm.

The programmes of thermal treatment given in Fig. 2 were applied for sintering in order to check if there are conditions for achieving single phase or less decomposed ceramics, respectively. The different times of keeping at 200 and 400°C for 1 and for 10 h at the sintering temperature of 1250, 1300 or 1350°C are indicated in the diagram and also cooling without (programme I) or with annealing at 1000°C for 17 h (programme II and IIa) or 50 h (programme IIb and IIc).

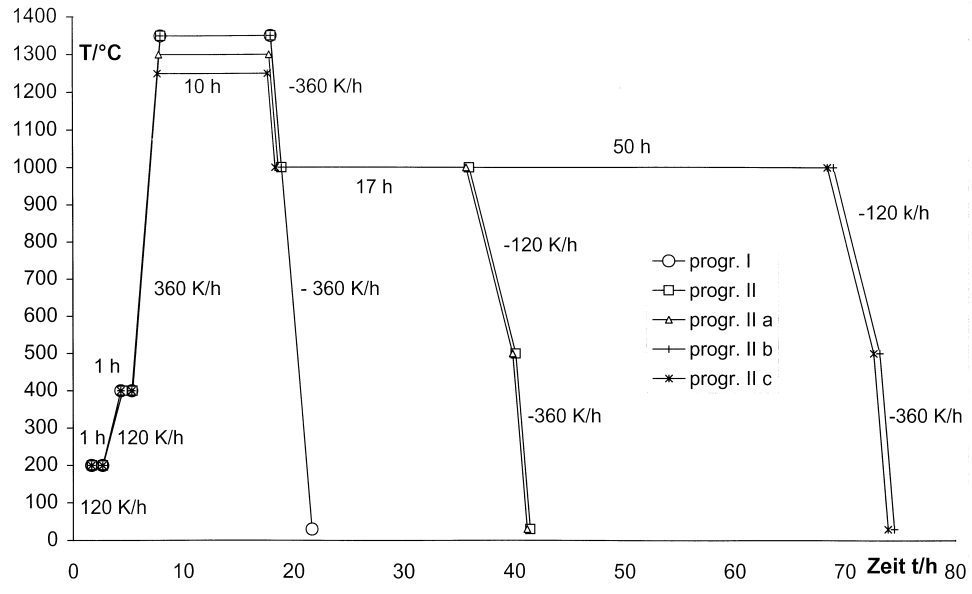

Fig. 2. The five different sintering programmes applied to the samples.

4. Structure of the prepared samples

X-ray diffraction measurements of the powdered ceramic samples confirm spinel formation as a result of sintering at 1350°C. However, only in a comparatively narrow area around the composition $FeNi_{0.5}Mn_{1.5}O_4$ ($a_0 = 842.8$ 4 pm) and $FeNi_{0.7}Mn_{1.3}O_4$ ($a_0 = 840.7$ 4 pm) is single-phase spinel formation observed. Some of the diffraction peaks of the other samples are split indicating the presence of a NiO phase which is formed at the high sintering temperature the more the closer the composition is to the borderline $NiMn_2O_4$–$NiFe_2O_4$ in the diagram of Fig.1.

Moreover, chemical analyses of the samples make it possible to reveal the phase constitution of the sintered ceramics, because there is a close relation between the residual oxidation equivalents, the share of NiO and the composition of the spinel in the mixture of phases.

For this purpose, powdered ceramic samples are dissolved in a solution of Fe^{II} of known content in hydrochloric acid using a closed vessel with an inert atmosphere of nitrogen or argon. According to the formula $Fe^{III}_x Ni^{II}_y Mn^z_{3-x-y}O_4$ the oxidation equivalents $k = z - 2 = (2 - x)/(3 - x - y)$ (z is the average oxidation number of Mn) will be transferred to Fe^{II} yielding Fe^{III}, which opens the possibility to titrate the residual Fe^{II} ion concentration, e.g. potentiometrically using a Ce^{IV} solution of known molarity. If oxygen loss according to Eq. (5a) with the formula $Fe^{III}_x Ni^{II}_y Mn^z_{3-x-y}\ O_{3+x/2+\delta}$ occurs, the relation $k = z - 2 = 2\delta/(3 - x - y)$ has to be taken into account, i.e. at known values of x and y from the analytically determined value of k it is always possible to check the oxygen loss $[(2 - x - 2\delta)/4]\ O_2$ which has occurred during sintering. However, the true structure of the ceramic is not a single phase anion defect spinel. Actually, the reaction given by Eq. (5b) is responsible for decomposition at sintering.

$$Fe^{III}_x Ni^{II}_y Mn^z_{3-x-y}O_4 \rightarrow Fe^{III}_x Ni^{II}_y Mn^z_{3-x-y}O_{3+x/2+\delta} + \frac{2-x-2\delta}{4}O_2 \quad (5a)$$

$$Fe^{III}_x Ni^{II}_y Mn^z_{3-x-y}O_4 \rightarrow a\,NiO + \frac{3-a}{3} Fe^{III}_{\frac{3x}{3-a}} Ni^{II}_{\frac{3(y-a)}{3-a}} Mn^{II}_{\frac{3(3-x-y)}{3-a}} Mn^{z}_{4} + a/6\ O_2 \quad (5b)$$

It is possible to separate the average oxidation number z into fractions of Mn^{II} and Mn^{III}, e.g. for $x = y = 1$ the molar unit $M = [a\ NiO + \frac{3-a}{3} Fe^{III}_{\frac{3}{3-a}} Ni^{II}_{\frac{3(1-a)}{3-a}} Mn^{II}_{\frac{2a}{3-a}} Mn^{III}_{\frac{3-2a}{3-a}} O_4]$ is representive for the ceramic powder sample. Hence, starting the analysis with the weight m, it is easy to find the relation $p = \frac{m}{M}(1 - \frac{2}{3}a)$ giving the number of oxidation equivalents which appear as Mn^{III} in the sample. These can be determined by the reaction with Fe^{II} during dissolution followed by titration with a Ce^{IV} solution.

The analytical data are summarized in Table 1 for ceramic samples, whose integral formulae are noted in the diagram of Fig. 1. As for $FeNiMnO_4$, undecomposed spinels are in the whole area accessible by application of the mixed crystal oxalate preparation route which makes possible sintering at 950 or 1000°C. However, following the mixed oxide preparation route, higher temperatures up to 1350°C are necessary. At these conditions only ceramic samples of $FeNi_{0,5}Mn_{1.5}O_4$ (sample 3) and $FeNi_{0.7}Mn_{1.3}O_4$ (sample 2) are found to exist in good approximation in the single-phase spinel state. The real state of all of the other samples sintered at 1350 or 1300°C is given by a mixture of NiO and a residual spinel with decreased content of NiO. For $FeNiMnO_4$ (sample 1), after decomposition at 1250 or 1350°C even the conditions of 50 h soaking at 1000°C in air (sintering program IIb and IIc) do not allow to restore the homogeneous spinel state according to the back reaction of Eq. (5b). A substantial part of NiO remains thus leading to a residual spinel with the ratio $Mn^{II}/Mn^{III} = 0.33 \pm 0.03$. Sample 4 is, after 2 and 3, the best approximation to a single-phase spinel state after sintering at 1350°C, provided that annealing at 1000°C for 17 h (sintering program II) is applied. However, the ratio Mn^{II}/Mn^{III} ist still 0.22 instead of 0.091 which is expected for the single phase spinel state. It is noteworthy that samples 7 and 8 with $Mn^{II}/Mn^{III} = 0.22$ and 0.25 separate just sufficient NiO to provide a residual spinel whose composition is close to the spinel which has already been found for sample 4. In accordance with the diagram of Fig. 1 the shift of spinel composition caused by NiO separation is indicated by these results. The NiO separation controlled approximation to a residual spinel compound seems to be also valid for samples 5, 6 and 9 showing the ratio $Mn^{II}/Mn^{III} = 0.29 \pm 0.04$.

The density ρ was determined from weighing and geometrical measurement of 10 un-metallized cylindrical samples. The theoretical density ρ_{th} was deduced from X-ray diffraction measurements taking into account the fraction of NiO ($a_0 = 416.84$ pm) and the fraction of the spinel of modified composition which forms the second phase in the mixture. The values $\rho_{rel.} = \rho/\rho_{th}$. being a measure of the residual porosity of the samples are also given in Table 1.

5. Electrical properties and aging

Twenty-four specimens of every batch of preparation have been measured at 25 and 100°C yielding the average values of the specific electrical resistivity $\rho_{25°C}$ and of the constant $B_{25/100°C}$ which is a measure of thermistor sensitivity.

For aging, after initial measuring, a set of four samples was submitted to annealing in each case at the

Table 1
Composition of the ceramic samples after sintering: [a NiO + $\frac{3-a}{3}Fe^{III}_{\frac{3}{3-a}}Ni^{II}_{\frac{3(1-a)}{3-a}}Mn^{II}_{\frac{2a}{3-a}}Mn^{III}_{\frac{3-2a}{3-a}}O_4$] determined by oxidimetric titration

No.	x	y	Formula of the single-phase spinel prepared by the precursor route	Applied programme of sintering	Density $\rho_{rel.}$ (%)	Weighing out loss (m/mg)	Oxidation eqivalent $p_{measured}$	Relation of m and p to the NiO content a	Mol a of NiO in the decomposed state	Content in mol and composition of the spinel in the mixture
1	1	1	$Fe^{III}Ni^{II}Mn^{III}O_4$	I	99.8	246.4	0.73	$a=\frac{m-233.5p}{0.6667m-5.33p}$	0.474	$0.842Fe^{III}_{1.87}Ni^{II}_{0.625}MnII_{0.375}Mn^{III}_{0.814}O_4$
				II	99.6	225.5	0.745		0.352	$0.883Fe^{III}_{1.333}Ni^{II}_{0.734}Mn^{II}_{0.266}Mn^{III}_{0.867}O_4$
				IIa	99.4	255.2	0.810		0.398	$0.867Fe^{III}_{1.153}Ni^{II}_{0.694}Mn^{II}_{0.306}Mn^{III}_{0.847}O_4$
				IIb	99.3	254.1	0.807		0.398	$0.867Fe^{III}_{1.153}Ni^{II}_{0.694}Mn^{II}_{0.306}Mn^{III}_{0.847}O_4$
				IIc	99.2	259.9	0.863		0.347	$0.884Fe^{III}_{1.131}Ni^{II}_{0.738}Mn^{II}_{0.262}Mn^{III}_{0.869}O_4$
			from $FeNiMn(C_2O_4)_3{*}6H_2O$	1000°C	85	250,0	1,071		0	$1.00Fe^{III}Ni^{II}Mn^{III}O_4$
2	1	0.7	$Fe^{III}Ni^{II}_{0.7}Mn^{II}_{0.3}Mn^{III}_{1.3}O_4$	I	98.8	257.2	1.051	$a=\frac{m-233.4p}{0.667m-5.33p}$	0.0072	$0.976Fe^{III}_{1.025}Ni^{II}_{0.643}Mn^{II}_{0.357}Mn^{III}_{0.975}O_4$
				II	98.8	252.9	1.074		0.014	$0.995Fe^{III}_{1.005}Ni^{II}_{0.689}Mn^{II}_{0.311}Mn^{III}_{0.995}O_4$
3	1	0.5	$Fe^{III}Ni^{II}_{0.5}Mn^{II}_{0.5}Mn^{III}_{1.0}O_4$	I	94.2	248.8	1.069	$a=\frac{m-231.6p}{0.667m-5.33p}$	0.0075	$0.998Fe^{III}_{1.003}Ni^{II}_{0.495}Mn^{II}_{0.508}Mn^{II}_{0.997}O_4$
				II	95.8	255.2	1.088		0.019	$0.994Fe^{III}_{1.006}Ni^{II}_{0.485}Mn^{II}_{0.515}Mn^{III}_{0.996}O_4$
4	0.291	0.846	$Fe^{III}_{0.29}Ni^{II}_{0.85}Mn^{II}_{0.155}Mn^{III}_{1.71}O_4$	I	99.8	157,6	1.000	$a=\frac{m-234.6p}{0.667m-5.33p}$	0.348	$0.884Fe^{III}_{0.329}Ni^{II}_{0.563}Mn^{II}_{0.437}Mn^{III}_{1.671}O_4$
				II	99.9	151,5	0.995		0.266	$0.991Fe^{III}_{0.319}Ni^{II}_{0.636}Mn^{II}_{0.364}Mn^{III}_{1.681}O_4$
5	0.708	0.843	$Fe^{III}_{0.71}Ni^{II}_{0.84}Mn^{II}_{0.16}Mn^{III}_{1.29}O_4$	I	99.6	157.0	0.910	$a=\frac{m-232.8p}{0.667m-5.33p}$	0.338	$0.887Fe^{III}_{0.798}Ni^{II}_{0.569}Mn^{II}_{0.431}Mn^{III}_{1.202}O_4$
				II	99.8	207.1	0.980		0.298	$0.901Fe^{III}_{0.786}Ni^{II}_{0.605}Mn^{II}_{0.395}Mn^{III}_{1.214}O_4$
6	0.64	1.00	$Fe^{III}_{0.64}Ni^{II}_{1.00}Mn^{III}_{1.36}O_4$	I	99.8	200.2	0.889	$a=\frac{m-233.2p}{0.667m-5.33p}$	0.507	$0.831Fe^{III}_{0.769}Ni^{II}_{0.600}Mn^{II}_{0.400}Mn^{III}_{1.231}O_4$
				II	99.8	195.6	0.925		0.402	$0.866Fe^{III}_{0.738}Ni^{II}_{0.696}Mn^{II}_{0.304}Mn^{III}_{1.262}O_4$
7	0.27	1.00	$Fe^{III}_{0.27}Ni^{II}_{1.00}Mn^{III}_{1.73}O_4$	I	99.8	155.2	0.913	$a=\frac{m-233.3p}{0.667m-5.33p}$	0.568	$0.811Fe^{III}_{0.333}Ni^{II}_{0.533}Mn^{II}_{0.467}Mn^{III}_{1.667}O_4$
				II	99.8	150.4	0.928		0.465	$0.845Fe^{III}_{0.319}Ni^{II}_{0.634}Mn^{II}_{0.366}Mn^{III}_{1.681}O_4$
8	0.21	1.14	$Fe^{III}_{0.21}Ni^{II}_{1.14}Mn^{III}_{1.51}Mn^{IV}_{0.14}O_4$	I	99.7	156.4	0.875	$a=\frac{m-233.6p}{0.667m-5.33p}$	0.762	$0.746Fe^{III}_{0.281}Ni^{II}_{0.507}Mn^{II}_{0.493}Mn^{III}_{1.719}O_4$
					99.6	158.6	0.915		0.700	$0.767Fe^{III}_{0.274}Ni^{II}_{0.575}Mn^{II}_{0.425}Mn^{III}_{1.726}O_4$
9	0.51	1.14	$Fe^{III}_{0.51}Ni^{II}_{1.14}Mn^{III}_{1.21}Mn^{IV}_{0.14}O_4$	I	99.5	176.6	0.746	$a=\frac{m-233.6p}{0.667m-5.33p}$	0.782	$0.740Fe^{III}_{0.69}Ni^{II}_{0.485}Mn^{II}_{0.515}Mn^{III}_{1.31}O_4$
				II	99.7	176.6	0.801		0.669	$0.777Fe^{III}_{0.656}Ni^{II}_{0.606}Mn^{II}_{0.394}Mn^{III}_{1.344}O_4$

temperature of 80, 100, 150, 200, 300 and 500°C as shown by the scheme of Fig. 3. After soaking for 72 h, the samples were removed from the thermostat for cooling in air, which involves conditions of rapid cooling. Measuring of the electrical restistivity at 25 and 100°C was carried out and annealing was proceeded at the same temperatures for up to 144 h and additionally followed by measuring again. The differences to the initial data lead to the $\Delta\rho_{25°C}/\rho_{25°C}$ values which indicate aging.

In order to check if aging is irreversible with time or if the changes $\Delta\rho_{25°C}/\rho_{25°C}$ are repeatable, all of the samples aged in a first cycle were submitted to annealing at 650°C for 10 h followed by cooling with a defined rate of −360 K/h (Fig. 3). Again, the electrical resitivity at 25 and 100°C of all of the 24 samples has been measured yielding the starting values $\rho_{25°C}(a)$ and $B_{25/100°C}(a)$ for the next annealing cycle which involved exactly the same steps of temperature for soaking 72 and 144 h as before. After that, heating at 650°C for 10 h has again been applied yielding the data $\rho_{25°C}(b)$ and $B_{25/100°C}(b)$ followed by repeating the aging programme for a third time.

According to these three cycles, Fig. 4a shows the values of aging $\Delta\rho_{25°C}/\rho_{25°C}$ and of $B_{25/100°C}$ for the spinel compound $FeNi_{0.5}Mn_{1.5}O_4$ (sample 3) prepared by sintering using programme II. Above 150°C, this ceramic compound with the single-phase structure exhibits extreme aging. The effects depend on the cooling rate applied in the last thermal treatment before measuring, because there is a remarkable difference between the intitial values $\rho_{25°C}=950$ kΩcm and $B_{25/100°C}=5023$ K and the data $\rho_{25°C}(a)=1212$ kΩcm and $B_{25/100°C}(a)=5052$ K obtained after the first period of heating at 650°C followed by defined cooling. Comparison of the data of the second and third cycle of aging indicates that these differences approximately vanish. The values of $\rho_{25°C}(b)=1200$ kΩcm and $B_{25/100°C}(b)=5056$ K are close to $\rho_{25°C}(a)$ and $B_{25/100°C}(a)$. Indeed, aging shown by the values of $\Delta\rho_{25°C}/\rho_{25°C}$ and $B_{25/100°C}$ in the diagram of Fig. 4a seems repeatable. Similar data of the electrical properties are observed after equilibration at 650°C provided that a defined cooling rate is used.

Frozen-in non-equilibrium states have to be assumed because of the applied conditions of cooling after sintering and also as a result of the rate of −360 K/h after keeping at 650°C. Therefore, samples were submitted to a long time annealing programme with +320 K/h up to 650°C, keeping for 2 h and cooling with −10 K/h down to 500°C and with −1.5 K/h to 50°C, i.e. cooling to room temperature was carried out within 13 days in order to achieve equilibrium as complete as possible.

The results are shown in Fig. 4b. In comparison to Fig. 4a the initial value is increased by a factor of about 2.4 in the result of the long time annealing treatment yielding a value of $\rho_{25°C}=2264$ kΩcm. However, and different from Fig. 4a the increase of $\Delta\rho_{25°C}/\rho_{25°C}$ and $B_{25/100°C}$ above 200°C fails. The values drop immediately when heating at 300°C is used. At 500°C the specific resistivity drops to 810 kΩcm which is close to 840 kΩcm measured for samples without long time annealing as shown in Fig. 4a.

This behavior suggests internal equilibria of a re-distribution of Mn^{II} and Fe^{III} cations between the tetrahedral and octahedral sites, which occur when the temperature changes. Both of the cations have a zero value of crystal field stabilization energy because of spherical d^5 electon configuration. $FeNi_{0.5}Mn_{1.5}O_4$ is a ferrimagnetic compound showing a Curie temperature of 245±5°C. Presumably, when this temperature is

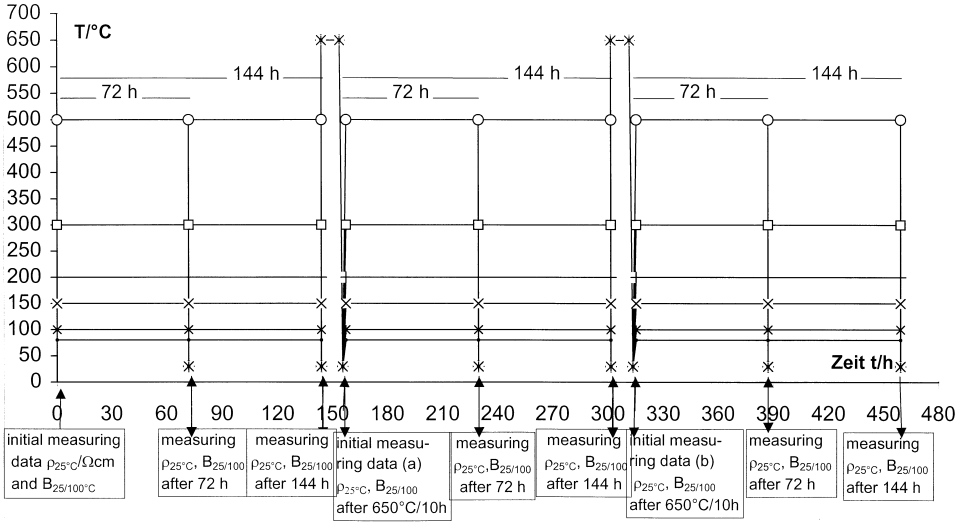

Fig. 3. Scheme of three cycles of annealing at 80, 100, 150, 200, 300 and 500°C starting for 72 h after measuring of $\rho_{25°C}/(\Omega cm)$ and $B_{25/100°C}$ and followed by again measuring and proceeded annealing up to altogether 144 h and repeating measuring. Equilibration follows at 650°C for 10 h before the second cycle starts.

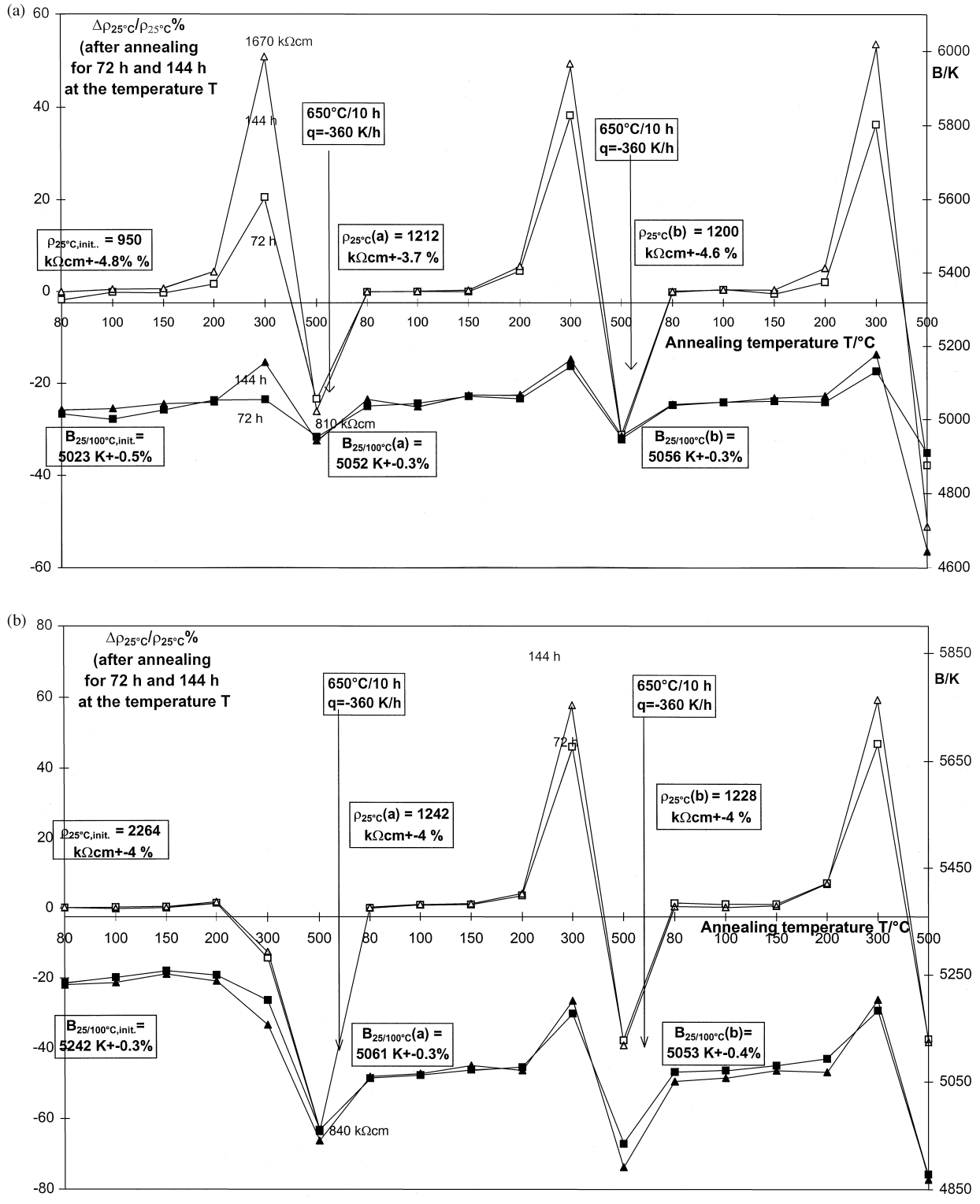

Fig. 4. Values $\triangle\rho_{25°C}/\rho_{25°C}$ and $B_{25/100°C}$ of aging of ceramic samples of $FeNi_{0.5}Mn_{1.5}O_4$ (sample 3) sintered at 1350°C according to programme II after annealing at the temperatures 80, 100, 150, 200, 300 and 500°C for 72 and 144 h: (a) rapidly cooled after sintering; (b) additionally submitted to a long time cooling treatment (13 days). The first annealing cycle of aging is repeated after soaking of all of these samples at 650°C for 10 h and after that followed by a third time.

approached and particularly in the paramagnetic state, cation re-distribution is kinetically favoured. The following equilibria appear plausible.

$$\left[Fe^{III}_{0.5}Mn^{II}_{0.5}\right]^{[4]}\left[Ni^{II}_{0.5}Fe^{III}_{0.5}Mn^{III}\right]^{[6]}O_4\ (LT) \Longleftrightarrow \left[Fe^{III}_{0.5+\delta}Mn^{II}_{0.5-\delta}\right]^{[4]}\left[Ni^{II}_{0.5}Fe^{III}_{0.5-\delta}Mn^{II}_{\delta}Mn^{III}\right]^{[6]}O_4\ (HT) \quad (6a)$$

with $0 < \delta < 0.5$ or

$$\left[Fe^{III}_{0.5}Mn^{II}_{0.5}\right]^{[4]}\left[Ni^{II}_{0.5}Fe^{III}_{0.5}Mn^{III}\right]^{[6]}O_4\ (LT) \Longleftrightarrow \left[Fe^{III}_{0.5-m}Mn^{II}_{0.5+m}\right]^{[4]}\left[Ni^{II}_{0.5}Fe^{III}_{0.5+m}Mn^{IV}_{m}Mn^{III}_{1-2m}\right]^{[6]}O_4 \quad (6b)$$

including partial Mn^{III} disproportionation with $0 < m < 0.5$. The combination of Eq. (6a) and (6b) is unlikely because at crystallographically equivalent octahedral sites Mn^{II} and Mn^{IV} should always form 2 Mn^{III}. Different equilibrium states characterized by δ or m have to be assumed as a function of temperature thus producing changes of the concentration of sufficiently adjacent polaron states Mn^{II}/Mn^{III} or Mn^{III}/Mn^{IV}, respectively. They form the real concentration of charge carriers in the ceramics. Therefore changes of site occupation are expected to affect the pre-exponential factor of the Arrhenius relation and in part also the B constant. Lifting of ferrimangetic coupling by increasing the temperature seems to favour cation re-distribution towards equilibrium.

Quenching during the period of cooling after sintering leads at room temperature to a frozen-in state containing a higher concentration of polaron states yielding a lower resistivity than should be valid in the range of lower temperature, i.e. the quenched non-equilibrium state is more on the right hand side (HT) of Eq. (6a) or (6b) (δ or $m > 0$), respectively. Consequently, starting aging by increasing the temperature step by step from room temperature to higher temperature, first of all increasing resistivity values have to be expected because the relaxation towards equilibrium shifts Eq. (6a) or (6b) to the left hand side-(LT). However, when the Curie temperature is significantly exceeded, e.g. at 500°C, the polaron state concentration is increased with low relaxation thus yielding a shift to the right-hand side (HT) with a lowering of the value of resisitivity.

On the other hand, in the result of long time annealing, i.e. cooling to room temperature within 13 days, the low temperature state (LT) seems to be widely approached showing a significantly increased value of the electrical resistivity as shown in Fig. 4b. Consequently, starting from room temperature, heating generates already from the beginning growing values of the polaron state concentration, which leads to decreasing values of the electrical resistivity as soon as the relaxation time is sufficiently lowered by the temperature. Indeed, the equilibria of Eq. (6a) or (6b) are able to explain the cyclic behavior of aging in the range of temperature up to 400°C.

Analogous results have been obtained for $FeNi_{0.5}Mn_{1.5}O_4$ ceramic samples which were prepared by sintering using program I. As can be seen from Fig. 5a, due to omission of the step of soaking for 17 h at 1000 °C, the samples appear in a more quenched state. Therefore, the initial high value of the electrical resistivity is lowered to 792 kΩcm. The more the annealing cycles proceed, the more pronounced the changes of the electrical data during aging. Again the direct drop of the resistivity is observed as a result of long time annealing according to the 13 days programme described above (Fig. 5b).

As an example for heterogeneous ceramics, (Fig. 6a and 6b) show the results of aging for sample (1) whose integral formula is $FeNiMnO_4$. Mixed oxide preparation with sintering according to programme IIa yields a mixture of 0.398 mole NiO and 0,867 mole $Fe^{III}_{1,153-}Ni^{II}_{0.694}\ Mn^{II}_{0.306}Mn^{III}_{0.847}O_4$ (Table 1). The effects of aging are remarkably reduced. However, despite the heterogeneity which is representive for sintering at 1300°C followed by 17 h annealing at 1000°C, the changes of the electrical data during aging are also in good approximation repeatable as for the single-phase ceramic compound $FeNi_{0.5}Mn_{1.5}O_4$. The applied temperatures at aging and for annealing at 650°C are sufficiently below the temperature where the non-equilibrium state of the mixture of the two phases could be lifted. Because of failing thermal activation the back reaction which is given by Eq. (5b) cannot take place. Indeed, there is no recognizable shift of the electrical data in the result of annealing at 650°C.

Moessbauer measurements of ceramic samples of the cubic spinel compound $FeNiMnO_4$ in the single-phase state prepared by the precursor route, imply the cation site distribution $[Fe^{III}_{0.67}Mn^{II}_{0.33}]^4[Fe^{III}_{0.33}Ni^{II}Mn^{III}_{0.33}Mn^{IV}_{0.33}]^{[6]}O_4$.[17] This compound is also ferrimagnetic showing a Curie temperature of 287°C. Oxygen loss followed by NiO separation should be favoured because of the content of Mn^{IV}. In the decomposed state for the residual spinel the most probable cation site occupation is suggested to be near $[Fe^{III}_{0.694}Mn^{II}_{0.306}]^{[4]}[Fe^{III}_{0.459}Ni^{II}_{0.694}Mn^{III}_{0.847}]^{[6]}O_4$. This is expected to be a high resistivity low temperature state (LT). In close relation to Eqs. (6a) and (6b), this configuration makes it possible to assume decreasing values of the resistivity at higher temperature according to

$$\left[Fe^{III}_{0.694}Mn^{II}_{0.306}\right]^{[4]}\left[Fe^{III}_{0.459}Ni^{II}_{0.694}Mn^{III}_{0.847}\right]^{[6]}O_4\ (LT) \Longleftrightarrow \left[Fe^{III}_{0.694+\delta}Mn^{II}_{0.306-\delta}\right]^{[4]}\left[Fe^{III}_{0.459-\delta}Ni^{II}_{0.694}Mn^{II}_{\delta}Mn^{III}_{0.847}\right]^{[6]}O_4\ (HT) \quad (7a)$$

or, more likely,

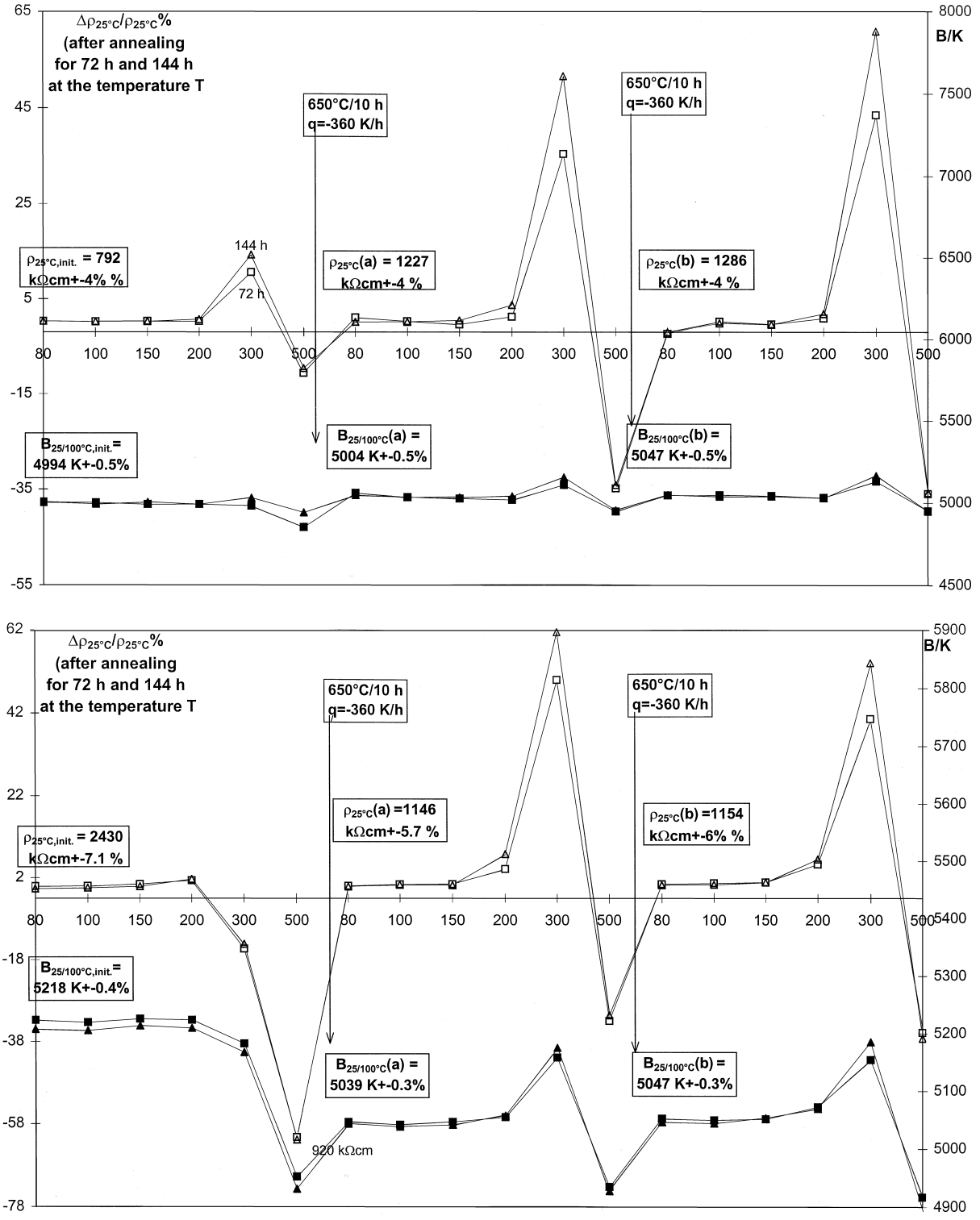

Fig. 5. Values $\triangle\rho_{25^\circ C}/\rho_{25^\circ C}$ and $B_{25/100^\circ C}$ of aging of ceramic samples of $FeNi_{0.5}Mn_{1.5}O_4$ (sample 3) sintered at 1350°C according to programme I after annealing at the temperatures 80, 100, 150, 200, 300 and 500°C for 72 and 144 h; (a) rapidly cooled after sintering; (b) additionally submitted to a long time cooling treatment (13 days). The first annealing cycle of aging is repeated after soaking of all of these samples at 650°C for 10 h and after that followed by a third time.

Table 2
Electrical properties of the samples [a $NiO + \frac{3-a}{3} Fe^{III}_{\frac{3}{3-a}} Ni^{II}_{\frac{3(1-a)}{3-a}} Mn^{II}_{\frac{2a}{3-a}} Mn^{III}_{\frac{3-2a}{3-a}} O_4$], initial data and values (a) and (b) after annealing and heating at 650°C

No.	Applied programme of sintering	Mol a of NiO in the ceramic samples	Content in mol and composition of the spinel in the ceramic samples after sintering at 1350 or 1300°C	$\rho_{25°C,\ init.}$ (kΩcm)	$B_{25/100°C,init}$ (K) (%)	$\rho_{25°C}$ (a) (kΩcm)	$B_{25/100°C}(a)$ (K) (%)	$\rho_{25°C}(b)$ (kΩcm)	$B_{25/100°C}$ (b) (K) (%)
1	I	0.474	$0.842\ Fe^{III}_{1.187}Ni^{II}_{0.625}Mn^{II}_{0.375}Mn^{III}_{0.814}O_4$	125.8±3.6	4118±0.2	134.9±4.0%	4103±0.6%	135.4±3.5	4127±0.2
	II	0.352	$0.883Fe^{III}_{1.133}Ni^{II}_{0.734}Mn^{II}_{0.266}Mn^{III}_{0.867}O_4$	70.6±4.2	3920±0.24	72.8±4.3	3919±0.27	72.7±4.3	3921±0.3
	IIa	0.398	$0.867Fe^{III}_{1.153}Ni_{0.694}Mn^{II}_{0.306}Mn^{III}_{0.847}O_4$	43.3±2.2	3874±0.13	45.0±2.3	3877±0.14	45.1±2.3	3881±0.13
	1000°C	0	$1.00Fe^{III}Ni^{II}Mn^{III}O_4$	6.80±1.4	3398±0.21	–	–	–	–
2	I	0.072	$0.976Fe^{III}_{1.025}Ni^{II}_{0.643}Mn^{II}_{0.357}Mn^{II}_{0.357}Mn^{III}_{0.975}O_4$	56.6±4.0	4113±1.2	60.1±4.2	4123±1.3	60.7±4.3	4122±1.3
	II	0.014	$0.995Fe^{III}_{1.005}Ni^{II}_{0.689}Mn^{II}_{0.311}Mn^{III}_{0.995}O_4$	30.1±4.0	3972±0.4	30.6±4.3	3974±0.4	30.8±4.2	3974±0.4
3	I	0.0075	$0.998Fe^{III}_{1.003}Ni^{II}_{0.495}Mn^{II}_{0.508}Mn^{III}_{0.997}O_4$	792±4.0	4994±0.5	1227±4.0	5004±0.5	1286±4.0	5047±0.5
	II	0.019	$0.994Fe^{III}_{1.006}Ni_{0.485}Mn^{II}_{0.515}Mn^{III}_{0.996}O_4$	950±4.8	5023±0.5	1212±3.7	5052±0.3	1200±4.6	5056±0.3
4	I	0.348	$0.884Fe^{III}_{0.329}Ni^{II}_{0.563}Mn^{II}_{0.437}Mn^{III}_{1.671}O_4$	11.2±2.6	4044±0.3	11.0±5.0	4025±0.4	–	–
	II	0.266	$0.991Fe^{III}_{0.319}Ni^{II}_{0.636}Mn^{II}_{0.364}Mn^{III}_{1.681}O_4$	6.1±4.8	3922±0.3	6.2±5.0	3915±0.5	6.2±4.9	3906±0.9
5	I	0.338	$0.887Fe^{III}_{0.798}Ni^{II}_{0.569}Mn^{II}_{0.431}Mn^{III}_{1.202}O_4$	29.1±6.0	3986±0.7	30.0±6.0	3982±0.7	–	–
	II	0.298	$0.901Fe^{III}_{0.786}Ni^{II}_{0.605}Mn^{II}_{0.395}Mn^{III}_{1.214}O_4$	13.9±5.8	3821±0.5	14.0±5.9	3820±0.5	14.0±5.9	3818±6.0
6	I	0.507	$0.831Fe^{III}_{0.769}Ni^{II}_{0.600}Mn^{II}_{0.400}Mn^{III}_{1.231}O_4$	14.75±5	3807±0.7	14.72±6.0	3799±07	14.86±6.0	3802±0.7
	II	0.402	$0.866Fe^{III}_{0.738}Ni^{II}_{0.696}Mn^{II}_{0.304}Mn^{III}_{1.262}O_4$	13.70±0.6	3731±0.6	13.75±5.0	3725±0.6	13.68±6.0	3718±0.6
7	I	0.568	$0.811Fe^{III}_{0.333}Ni^{II}_{0.533}Mn^{II}_{0.467}Mn^{III}_{1.667}O_4$	7.31±6.0	3935±0.7	7.12±6.0	3921±0.7	6.98±6.0	3912±0.7
	II	0.465	$0.845Fe^{III}_{0.319}Ni^{II}_{0.634}Mn^{II}_{0.366}Mn^{III}_{1.681}O_4$	4.74±5.8	3837±0.5	4.73±5.9	3833±0.5	4.63±5.9	3825±6.0
8	I	0.762	$0.746Fe^{III}_{0.281}Ni^{II}_{0.507}Mn^{II}_{0.493}Mn^{III}_{1.719}O_4$	8.59±6.0	3970±0.7	8.40±6.0	3958±0.7	8.13±6.0	3948±0.7
	II	0.700	$0.767Fe^{III}_{0.274}Ni^{II}_{0.575}Mn^{II}_{0.425}Mn^{III}_{1.726}O_4$	5.36±5.7	3876±0.5	5.36±5.9	3873±0.5	5.32±5.7	3869±5.0
9	I	0.782	$0.740Fe^{III}_{0.69}Ni^{II}_{0.485}Mn^{II}_{0.515}Mn^{III}_{1.31}O_4$	25.7±3.7	3880±0.13	25.7±3.6	3864±0.2	25.1±4.7	3852±0.5
	II	0.669	$0.777\ Fe^{III}_{0.656}Ni^{II}_{0.606}Mn^{II}_{0.394}Mn^{III}_{1.344}O_4$	12.8±3.33	3719±0.09	12.7±3.4	3708±0.13	12.4±5.4	3673±1.3

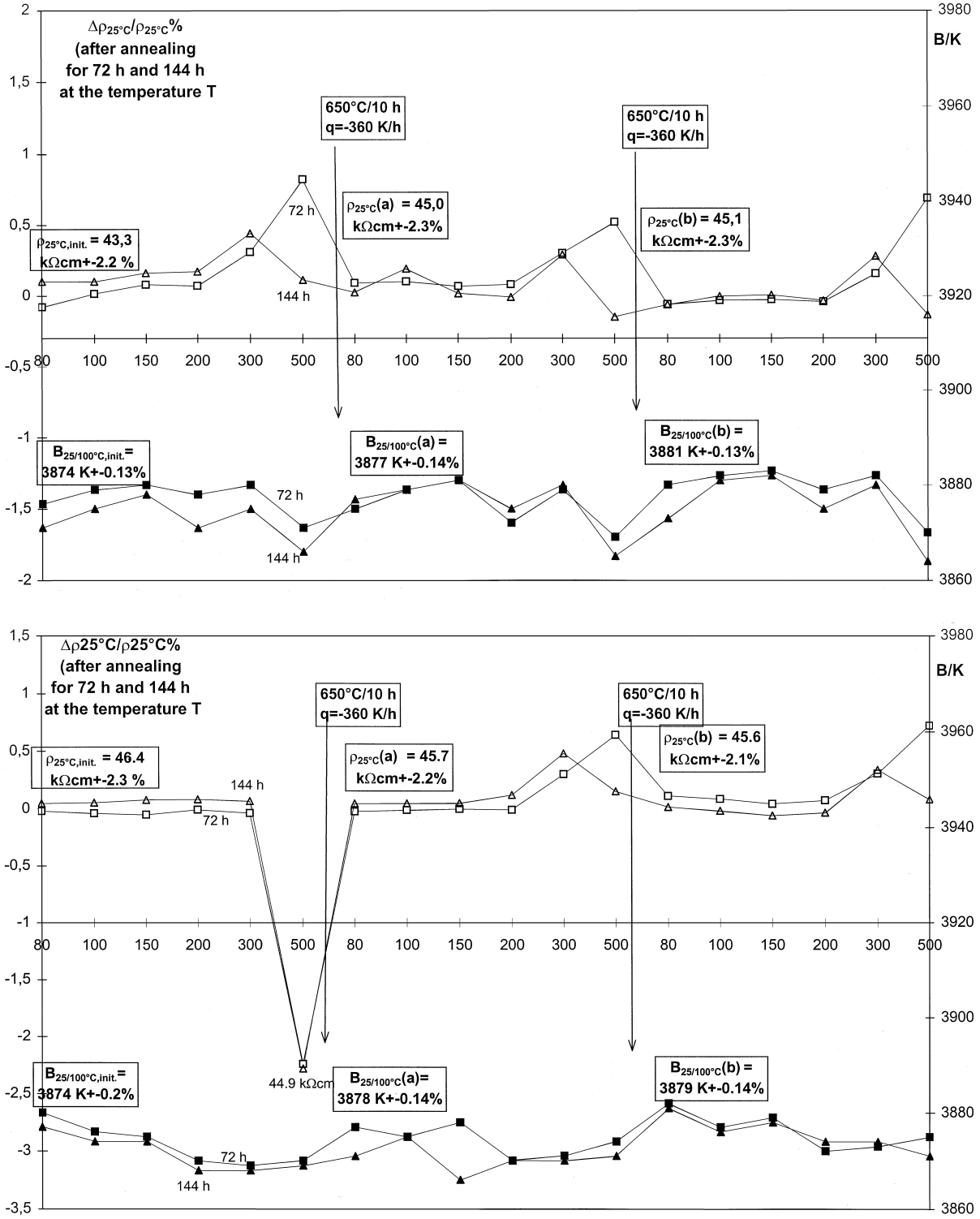

Fig. 6. Values $\triangle\rho_{25^\circ C}/\rho_{25^\circ C}$ and $B_{25/100^\circ C}$ of aging of ceramic samples sintered at 1300°C according to programme II a (sample 1) consisting of a mixture of 0.398 mol NiO and 0.867 mol $Fe^{III}_{1.153}Ni^{II}_{0.694}Mn^{II}_{0.306}Mn^{III}_{0.847}O_4$ after annealing at the temperatures 80, 100, 150, 200, 300 and 500°C for 72 h and 144 h; (a) rapidly cooled after sintering; (b) additionally submitted to a long time cooling treatment (13 days). The first annealing cycle of aging is repeated after soaking of all of these samples at 650°C for 10 h and after that followed by a third time.

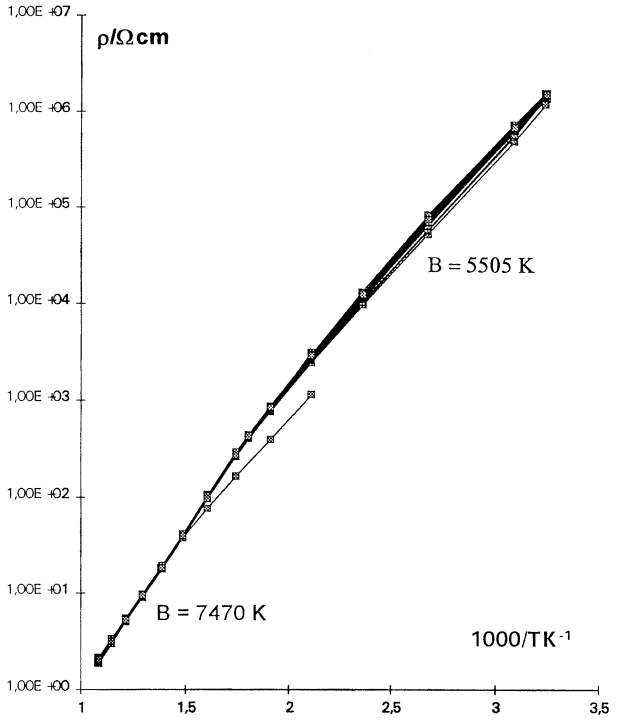

Fig. 7. The specific resistivity of $FeNi_{0.5}Mn_{1.5}O_4$ ceramic samples co-fired with Pt electrodes as a function of the reciprocal temperature in a semi-logarithmic plot of 18 heating up and down cycles showing relaxation in the low temperature range up to about 400°C and no aging effects above this temperature.

$$\left[Fe^{III}_{0.694}Mn^{II}_{0.306}\right]^{[4]}\left[Fe^{III}_{0.459}Ni^{II}_{0.694}Mn^{III}_{0.847}\right]^{[6]}O_4\ (LT) \Longleftrightarrow \left[Fe^{III}_{0.694-m}Mn^{II}_{0.306+m}\right]^{[4]} \left[Fe^{III}_{0.459+m}Ni^{II}_{0.694}Mn^{IV}_{m}Mn^{III}_{0.847-2m}\right]^{[6]}O_4\ (HT) \quad (7b)$$

The polaron state concentration is increasing from the left to the right hand side. With sufficiently rapid cooling, the high temperature configuration (HT) is at least partially quenched thus leading to an increase of the resistivity in the result of heating at 300°C for 72 or 144 h, respectively, which is shown in Fig. 6a. On the other hand, the shift to the right hand side of Eq. (7a) or (7b) is indicated in Fig. 6b showing the results of aging, which are observed again after the pre-treatment of long time annealing of the samples.

In Table 2, for all of the prepared samples the average values of the initial data $\rho_{25°C,init.}$ and $B_{25/100°C,init.}$ are collected together with the data $\rho_{25°C}(a)$ and $B_{25/100°C}(a)$ as well as $\rho_{25°C}(b)$ and $B_{25/100°C}(b)$ measured after the first and second step of soaking at 650°C, respectively.

The heterogeneous ceramics show the better stability in the low temperature range up to 150°C, which is satisfactory for most practical purposes. However, in the range up to about 400°C, aging appears as a phenomenon of relaxation of cation re-distribution towards equilibrium, which is reversible indicating an inherent behavior of spinel forming ceramics containing Mn^{II} and Fe^{III} cations. However, above the range of temperature where the electrical properties are submitted to time dependent relaxation, these disadvantages vanish. Actually, above temperatures of about 400°C, single-phase ceramics around the composition $FeNi_{0.5}Mn_{1.5}O_4$ do not show aging. Therefore, they should be suitable for NTC high temperature applications.

There are other spinels, e.g. $[Mg]^{[4]}[Ni^{II}Mn^{IV}]^{[6]}O_4$ or $[Mn^{II}]^{[4]}[Cr^{III}_2]^{[6]}O_4$, whose terahedral and octahedral site occupation should be pinned because of important differences of the values of the crystal field stabilization energy of the cations. Therefore, they are expected to be free from aging even at medium temperatures. At the same time, they are likely to show a high value of the B constant. However, $MgNiMnO_4$ decomposes already above 720°C in air by oxygen loss[18] which prevents ceramic densification. $MnCr_2O_4$ has the disadvantage of chromium oxide volatility on long time high temperature exposure in air.

6. High temperature thermistor ceramics $FeNi_{0.5}Mn_{1.5}O_4$

Fig. 7 shows the characteristic of a ceramic specimen of $FeNi_{0.5}Mn_{1.5}O_4$. The curve has been measured 18 times starting from room temperature up about 750°C and back. Indeed, in the low temperature range up to about 300°C relaxation effects prevail, which impairs application. The long waiting time for achieving a constant value of resistivity after changing the temperature cannot be accepted for practical purposes. On the other hand, above about 400°C the curves coincide indicating sufficiently short relaxation yielding an accurate correlation between temperature and electrical resistivity.

At the same time, above 400°C the $B_{25/100°C}$ constant is increasing, i.e. the thermistor sensitivity becomes improved. Presumably, in the high temperature range the exponent of Eq. (3) has to be completed by the driving force ΔG of polaron formation having a positive sign. Indeed, the law of mass action controls the polaron state concentration which lowers the resistivity at increasing temperature.

$$\rho(T) = \rho(25°C)e^{-\frac{\Delta S}{R}}e^{\frac{\Delta H+E_A}{RT}} \quad (8)$$

Interpreting the difference 7470−5505 = 1965 K as caused by polaron state formation leads to a value of 16.3 kJ/mole for the enthalpy of the reaction given by Eq. (6a) or (6b), respectively. Schmalzied[19] measured 10.9 kJ/mol for the high temperature cation re-distribution of $NiAl_2O_4$ from the inversed configuration $[Al]^{[4]}[NiAl]^{[6]}O_4$ to random distribution $[Al_{2/3}Ni_{1/3}]^{[4]}[Ni_{2/3}Al_{4/3}]^{[6]}O_4$.

Supported by this additional term of enthalpy the temperature dependent thermistor sensitivity is increased yielding in the range of 750°C $\alpha = B/T^2 = 7470/1023^2 = 0.8\%$. In the high temperature range, the electrical properties of semiconducting ceramics based on $FeNi_{0.5}Mn_{1.5}O_4$ do not show aging. For the compound $Sr_7Mn_4O_{15}$ with $B = 14350$ K a sensitivity of 1.5% had been found even at 700°C.[20]

Acknowledgements

The authors are indebted to Mrs. Margarethe Pölzl for careful preparation and Mrs. Monika Kogler for measuring of the electrical data and aging of samples.

References

1. Siemens Matsushita Components. Keramische Bauelemente, A-8530 Deutschlandsberg, *Data Book*. 1996.
2. Keystone Carbon Company, Thermistor Division. *High-Temperature NTC Glass Encapsulated Thermistors*. St. Marys, PA 15857, USA.
3. Ishikawa, K., Tamai, T., Kanasashi M., Miyama M. and Hata, T., *Thermistor Sensor for Automotive Uses*. National Technical Report, Vol.34, 1988, pp.25–34.
4. Katsuki, N.,Tamal T., Moriwake H., LeGare J. and Yoshida S., Exhaust Gas High Temperature Sensor for LEV/ULEV and OBD Systems. SAE Technical Papers 960336. Int. Congr. & Expos. Detroit, MI, February 1996.
5. Wickham, J. D., Solid-phase equilibria in the system NiO–Mn_2O_3–O_2. *J. Inorg. Nucl. Chem*., 1964, **26**, 1369- 1377.
6. Schmalzried, H., Temperaturabhängigkeit der Kationenverteilung im Spinell $NiAl_2O_4$. *Naturwissenschaften*, 1960, **47**, 466.
7. Feltz, A., Töpfer, J. and Neidnicht, B., Untersuchungen an elektronenleitenden Oxid-systemen XXIII: Struktur und Eigenschaften stabiler Spinelle in den Reihen $M_zNiMn_{2-z}O_4$ (M = Li, Fe). *Zeitschr. Anorgan. Allg. Chem*., 1993, **619**, 39–46.
8. Martinez Sarrion, M. L. and Morales, M., Preparation and characterization of NTC thermistors based on $Fe_{2+\delta}Mn_{1-x-\delta}Ni_xO_4$. *J. Mater. Sci*., 1995, **30**, 2610–2615.
9. Feltz, A., Tendencies in the development and application of negative temperature coefficient oxide ceramics. In *Proceed. Electroceramics IV*, Vol. II, Aachen 1994, pp. 677–684.
10. Ricoult, D. L. and Schmalzried, H., Electrical conductivity of iron-doped NiO single crystal at equilibrium and during internal oxidation. *J. Am. Ceram. Soc*., 1987, **70**, 669–674.
11. Boucher, R., Buhl, R. and Perrin, M., Etude cristallographique du manganite spinelle cubique $NiMn_2O_4$ par diffraction de neutrons. *Acta Crystallogr., B25*, 2326–2333.
12. Brabers, V. A. M., van Setten, F. M. and Knapen, P. S. A., X-ray photoelectron spectroscopy study of the cation valencies in nickel managanite. *J. Solid State Chemistry*, 1983, **49**, 93–98.
13. Macklen, E. D., Electrical conductivity and cation distribution in nickel manganite. *J. Phys. Chem. Solids*, 1986, **47**, 1073–1079.
14. Töpfer, J., Feltz, A., Gräf, D., Hackl, B., Raupach, L. and Weissbrodt, P., Cation valencies and distribution in the spinels $NiMn_2O_4$ and $M_zNiMn_{2-z}O_4$ (M = Li, Cu) studied by XPS. *Phys. Status Solidi (a)*, 1992, **134**, 405–415.
15. Feltz, A. and Töpfer, J., Bildung von Defektspinellen und Phasenbeziehungen im System $NiMn_{3-x}O_4$. *Zeitschr. Anorgan. Allg. Chem*., 1989, **576**, 71–80.
16. Feltz, A. and Rosc, F. Sinterkeramik für hochstabile Thermistoren und Verfahren zu ihrer Herstellung. Patentschrift DE 4420657 A1, EP 0 678 656 A1.
17. Wartewig, P., Personal communication, Department of Physics, University Leipzig.
18. Feltz, A. and Seidel, A., Stabile Spinelle $Zn_zNiMn_{2-z}O_4$ und Vergleich mit Spinellen $Mg_zNiMn_{2-z}O_4$. *Zeitschr. Anorgan. Allg. Chem*., 1991, **608**, 166–172.
19. Schmalzried, H., Festkörperreaktionen. Akademieverlag, Berlin, 1973, p. 80.
20. Feltz, A., Kriegel, R. and Pölzl, W., $Sr_7Mn_4O_{15}$ ceramics for high temperature NTC thermistors. *J. Mater. Sci. Lett*., 1999, **18**, 1693–1695.